Modeling vibrational dephasing and energy relaxation of intramolecular anharmonic modes for multidimensional infrared spectroscopies

Akihito Ishizaki[a)] and Yoshitaka Tanimura[b)]
Department of Chemistry, Graduate School of Science, Kyoto University, Kyoto 606-8502, Japan

Starting from a system-bath Hamiltonian in a molecular coordinate representation, we examine an applicability of a stochastic multilevel model for vibrational dephasing and energy relaxation in multidimensional infrared spectroscopy. We consider an intramolecular anharmonic mode nonlinearly coupled to a colored noise bath at finite temperature. The system-bath interaction is assumed linear plus square in the system coordinate, but linear in the bath coordinates. The square-linear system-bath interaction leads to dephasing due to the frequency fluctuation of system vibration, while the linear-linear interaction contributes to energy relaxation and a part of dephasing arises from anharmonicity. To clarify the role and origin of vibrational dephasing and energy relaxation in the stochastic model, the system part is then transformed into an energy eigenstate representation without using the rotating wave approximation. Two-dimensional (2D) infrared spectra are then calculated by solving a low-temperature corrected quantum Fokker-Planck (LTC-QFP) equation for a colored noise bath and by the stochastic theory. In motional narrowing regime, the spectra from the stochastic model are quite different from those from the LTC-QFP. In spectral diffusion regime, however, the 2D line shapes from the stochastic model resemble those from the LTC-QFP besides the blueshifts caused by the dissipation from the colored noise bath. The preconditions for validity of the stochastic theory for molecular vibrational motion are also discussed. © *2006 American Institute of Physics.* [DOI: 10.1063/1.2244558]

I. INTRODUCTION

Ultrafast nonlinear spectroscopy plays a pivotal role in investigating inter- and intramolecular motions in complex molecular systems.[1] Over the last decade, extensive theoretical,[2–20] computational,[21–25] and experimental[26–35] efforts have been made for multidimensional vibrational spectroscopy to have a variety of information for molecular motion and interactions.

Owing to recent technological progresses in the generation of stable ultrashort infrared (IR) laser pulses, third-order spectroscopic experiments have been extended in the IR region and can, therefore, be utilized to investigate intramolecular vibrational transition rather than electronic one. As an intramolecular vibrational motion is sensitive to local fluctuation of surroundings, it provides an important window to insight into the structure and dynamics of complex molecules, solvents, and protein environments. While the line shapes observed in IR absorption spectroscopy are broadened due to static inhomogeneity, we can separate the contribution of homogeneous vibrational motion, which contains important microscopic dynamics, by third-order IR spectroscopy such as an IR photon echo measurement.[36] Theoretically, static inhomogeneity has been treated by using the slow modulation limit of the stochastic theory, and homogeneity by the fast modulation limit. However, there is also a wide intermediate range of modulation times between the inhomogeneous and homogeneous limits, which gives rise to what is called vibrational spectral diffusion. The spectral diffusion process was analyzed by means of three-pulse photon echo measurement. Hamm *et al.*[37] performed the first femtosecond IR three-pulse echo experiment on a mode of the azide ion N_3^- in deuterium water. Employing the stochastic theory of frequency fluctuation,[38,39] they quantified the magnitudes and time scales of dynamic solvent fluctuations that cause spectral diffusion. Hamm *et al.*[40] also achieved the first two-dimensional infrared (2D-IR) measurement by means of double-resonance or dynamic hole burning experiments on the amide I bands of *N*-methylacetamide and small globular peptides, and gained access to the detailed information on the structures of peptides that could not be obtained from linear absorption spectra. These works stimulated many experimental and theoretical studies[41–48] and sparked off the pulsed Fourier transform 2D-IR spectroscopy by means of the heterodyne-detected photon echo experiments.[49–52] Objects under study of 2D-IR spectroscopic experiments have definitely spread very wide: conformation and conformational fluctuations of small peptides[53–57] and dipeptides,[58,59] conformational changes in proteins,[60–63] hydrogen-bonded complexes,[64–67] and water dynamics.[68] In the immediate past, heterodyned *fifth*-order 2D-IR measurements[69] were reported on ions in glasses.[70,71]

In this paper, we explore roles of vibrational dephasing and energy relaxation involved in the multidimensional IR spectroscopy to establish a reasonable system-bath model to discuss these dissipative processes from a microscopic point of view. To study vibrational dephasing, the stochastic theory of transition frequencies was introduced[72] and intensively used to analyze the signals from IR echo and 2D-IR spectroscopy. The stochastic model was extensively utilized in

---

a)Electronic mail: ishizaki@kuchem.kyoto-u.ac.jp
b)Electronic mail: tanimura@kuchem.kyoto-u.ac.jp

125, 084501-1

the nuclear magnetic resonance (NMR) or electronically resonant spectroscopy.[39] The character of spectroscopic experiments is, however, different for vibrational and electronic transitions. While the decay time of population in electronically excited state is invariably long compared with the dephasing of optical transitions, that in vibrational excited states is sometimes comparable to the time scale of vibrational dephasing; the system relaxes toward the thermal equilibrium on time scale comparable with the vibrational dephasing. Nonetheless, the stochastic theory involves only frequency fluctuations without any accounts of the contributions from temperature and dissipation. Then, the effects of vibrational energy relaxation were sometimes included in a phenomenological manner independently from the stochastic theory. A simple one is a Bloch picture which accounts for the effects of energy relaxation and dephasing by a longitudinal relaxation time constant T_1, a transversal relaxation time constant T_2, and a pure dephasing time T_2^*, i.e., $1/T_2 = 1/2T_1 + 1/T_2^*$. The validity of such phenomenological approach is an open question, since such simple relation is based on the assumption of a weak coupling or a white noise bath within the rotating wave approximation (RWA). The stochastic theory and Bloch-Redfield theory also have inherent difficulty to treat a finite temperature system.

To clarify the above-mentioned problems, here, we start from a Hamiltonian consisting of an anharmonic molecular system coupled to a heat bath. The bath degrees of freedom are described by an ensemble of oscillators, which correspond to optically inactive modes such as solvent modes. The key to the relation between the coordinate and energy-level pictures is on a form of a system-bath interaction. To make our discussion more concrete, here, we denote the interaction potential between the vibrational mode of interest and the heat bath by $F(q,\{x_j\})$ as a function of vibrational coordinate q and the bath coordinates $\{x_j\}$, where x_j is the jth bath coordinate. We assume that $F(q,\{x_j\})$ can be expanded in q as follows:

$$F(q,\{x_j\}) = \frac{1}{1!}qF_1(\{x_j\}) + \frac{1}{2!}q^2F_2(\{x_j\}) + \cdots. \tag{1.1}$$

The second term in Eq. (1.1) alters the curvature of the potential energy surface $U(q)$ for vibrational motion in time for the evolution of $\{x_j\}$; hence, the system frequency is fluctuated on a time scale of bath dynamics. The first term with the linear dependence on q mainly gives rise to energy dissipation from the vibrational mode to the heat bath.[73,74] For anharmonic vibrational modes, the term also contributes to dephasing, i.e., anharmonicity-induced dephasing, due to the nonvanishing diagonal elements $\langle v|\hat{q}|v\rangle \neq 0$ $(v=0,1,2,\ldots)$, where $|v\rangle$ and $\langle v|$ are the vth energy eigenstate for modes and its Hermitian conjugate, respectively.

Starting from the coordinate representation of the system-bath interaction, we can identify the origin of vibrational dephasing and energy relaxation in the energy-level model. We calculate signals for coordinate model without employing such approximation as the RWA and compare the results with signals for an approximated expression of energy-level models. We then check the validity of the approximated Hamiltonian for various strengths of the system-

bath coupling and temperatures. The major difficulty to calculate signals for the system-bath Hamiltonian with interaction potential [Eq. (1.1)] is on the derivation of the equation of motion for a reduced density matrix. If temperature is high compared with vibrational excitation energy, one can use the quantum Fokker-Planck equation for nearly Markovian noise bath.[75] The case we want to discuss here is, however, the intramolecular vibrational modes, where the temperature is much lower than vibrational excitation energy; therefore, the system is regarded as in a low temperature where the quantum description of the system becomes important. For this purpose, we extended the quantum Fokker-Planck equation and included low-temperature correction terms.[76] We show how one can handle low-temperature system using this formalism. For the interaction potential in Eq. (1.1), we include terms up to the second order in q and take into account only the linear dependence on $\{x_j\}$, i.e., $F_1(\{x_j\}) = -v_{LL}\Sigma_j c_j x_j$ and $F_2(\{x_j\}) = -v_{SL}\Sigma_j c_j x_j$. Integrating the reduced equation of motion, we calculate 2D-IR signals and discuss the importance of dissipative and anharmonic effects which arise from the first term in Eq. (1.1) by comparison to the resultants from the energy-level picture with stochastic modulation.

This paper is organized as follows: In Sec. II we give a brief review of nonlinear optical responses and the stochastic theory. In Sec. III we introduce the quantum dissipative equation applicable to a low-temperature coordinate system, low-temperature corrected quantum Fokker-Planck (LTC-QFP) equation to analyze vibrational dephasing and energy relaxation in an intramolecular mode. In Sec. IV numerical results are presented as 2D-IR correlation spectra and are discussed. Finally, Sec. V is devoted to concluding remarks.

II. NONLINEAR RESPONSE FUNCTIONS

We consider a system consisting of a single intramolecular vibrational mode described by the Hamiltonian

$$\hat{H} = \frac{\hat{p}^2}{2m} + U(\hat{q}), \tag{2.1}$$

where m, q, p, and $U(\hat{q})$ denote the effective mass, the coordinate, the conjugate momentum, and the potential of the vibrational mode, respectively. Using the energy eigenstates of the system $\{|v\rangle\}$ $(v=0,1,\ldots,v_{max})$, we can rewrite Eq. (2.1) as

$$\hat{H} = \sum_{v=0}^{v_{max}} \hbar\omega_v |v\rangle\langle v|, \tag{2.2}$$

where $\hbar\omega_v$ is the energy of the vth eigenstate $|v\rangle$. We introduce transition frequencies between levels as $\omega_{jk} \equiv \omega_j - \omega_k$. As we will show below, the primary contribution of 2D-IR signals arises from the transitions between the lowest three energy levels. Then, the anharmonicity of the mode is expressed as

$$\Delta_{anh} \equiv \omega_{10} - \omega_{21}. \tag{2.3}$$

We assume that all other degrees of freedom, e.g., other internal modes or solvent modes, are optically inactive and

treat as a heat bath. The Hamiltonian of the system plus bath is denoted by $\hat{H}_{\text{tot}}$.

The first-order IR response function $R^{(1)}(t_1)$ is defined by[1]

$$R^{(1)}(t_1) = \frac{i}{\hbar}\langle [\hat{\mu}(t_1), \hat{\mu}(0)]\rangle, \qquad (2.4)$$

where $\hat{\mu}(t) \equiv e^{(i/\hbar)\hat{H}_{\text{tot}}t}\mu(\hat{q})e^{-(i/\hbar)\hat{H}_{\text{tot}}t}$ is the Heisenberg representation of the dipole-moment operator and $\langle\cdots\rangle$ $\equiv \text{Tr}\{\cdots\hat{\rho}_{\text{tot}}^{\text{eq}}\}$, with $\hat{\rho}_{\text{tot}}^{\text{eq}} = e^{-\beta\hat{H}_{\text{tot}}}/\text{Tr}\,e^{-\beta\hat{H}_{\text{tot}}}$. Using the hyperoperator notations,

$$\hat{O}^{\times}\hat{f} \equiv \hat{O}\hat{f} - \hat{f}\hat{O}, \quad \hat{O}^{\circ}\hat{f} \equiv \hat{O}\hat{f} + \hat{f}\hat{O} \qquad (2.5)$$

for any operator $\hat{O}$ and operand operator $\hat{f}$, we can recast Eq. (2.4) into

$$R^{(1)}(t_1) = \text{Tr}\left\{\mu(\hat{q})\hat{\mathcal{G}}(t_1)\frac{i}{\hbar}\mu(\hat{q})^{\times}\hat{\rho}_{\text{tot}}^{\text{eq}}\right\}, \qquad (2.6)$$

where $\hat{\mathcal{G}}(t)$ is the Liouville space propagator defined by $\hat{\mathcal{G}}(t)\hat{f} = e^{-(i/\hbar)\hat{H}_{\text{tot}}t}\hat{f}e^{(i/\hbar)\hat{H}_{\text{tot}}t}$ for any operator $\hat{f}$.

For resonant 2D-IR experiments, we consider the three pulses, tuned to the molecular vibration of interest, with wave vectors $\mathbf{k}_1$, $\mathbf{k}_2$, and $\mathbf{k}_3$ which are sequentially applied to samples. These pulses cross in a sample to generate a third-order polarization, which radiates a signal field in the phase-matched directions. The rephasing (echo) response detected in the direction $\mathbf{k}_I = +\mathbf{k}_3 + \mathbf{k}_2 - \mathbf{k}_1$ is described by the following correlation function:

$$
\begin{aligned}
&R_I^{(3)}(t_3, t_2, t_1) \\
&= \text{Tr}\left\{\hat{\mu}_{\leftarrow}\hat{\mathcal{G}}(t_3)\frac{i}{\hbar}\hat{\mu}_{\rightarrow}^{\times}\hat{\mathcal{G}}(t_2)\frac{i}{\hbar}\hat{\mu}_{\rightarrow}^{\times}\hat{\mathcal{G}}(t_1)\frac{i}{\hbar}\hat{\mu}_{\leftarrow}^{\times}\hat{\rho}_{\text{tot}}^{\text{eq}}\right\},
\end{aligned} \quad (2.7)
$$

where $\hat{\mu}_{\rightarrow}$ and $\hat{\mu}_{\leftarrow}$ are defined by

$$\hat{\mu}_{\rightarrow} \equiv \sum_v |v+1\rangle\mu_{v+1,v}\langle v|, \qquad (2.8a)$$

$$\hat{\mu}_{\leftarrow} \equiv \sum_v |v\rangle\mu_{v,v+1}\langle v+1|, \qquad (2.8b)$$

with the abbreviation $\mu_{j,k} = \langle j|\mu(\hat{q})|k\rangle$. The nonrephasing (virtual echo) response detected in the direction $\mathbf{k}_{II} = +\mathbf{k}_3 - \mathbf{k}_2 + \mathbf{k}_1$ is described by

$$
\begin{aligned}
&R_{II}^{(3)}(t_3, t_2, t_1) \\
&= \text{Tr}\left\{\hat{\mu}_{\leftarrow}\hat{\mathcal{G}}(t_3)\frac{i}{\hbar}\hat{\mu}_{\rightarrow}^{\times}\hat{\mathcal{G}}(t_2)\frac{i}{\hbar}\hat{\mu}_{\leftarrow}^{\times}\hat{\mathcal{G}}(t_1)\frac{i}{\hbar}\hat{\mu}_{\rightarrow}^{\times}\hat{\rho}_{\text{tot}}^{\text{eq}}\right\}.
\end{aligned} \quad (2.9)
$$

Note that the directions of the subscript arrows in Eqs. (2.7)–(2.9) correspond to those of the arrows depicted in Fig. 1.

These expressions provide us an intuitive picture upon the response function. For instance, the right-hand side of Eq. (2.6) can be read from right to left as follows. The thermal equilibrium state is modified by the first interaction with a laser pulse via the dipole moment at time $t=0$, and then it evolves in time for the interval t_1 by the propagator $\hat{\mathcal{G}}(t)$.
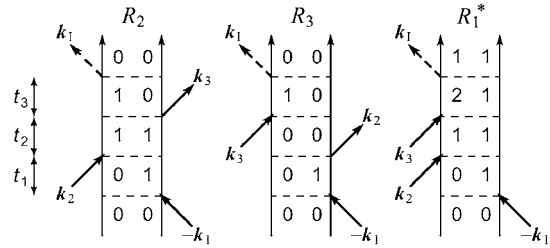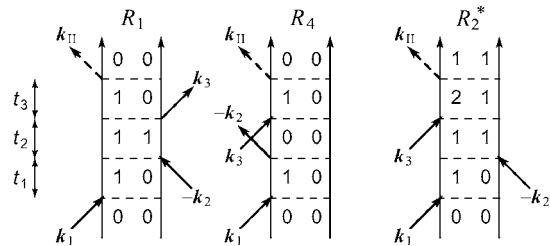

FIG. 1. The double-sided Feynman diagrams contributing to the (a) rephasing and (b) nonrephasing Liouville space pathways. The variables t_n ($n = 1,2,3$) represent the delays between the three input pulses to generate a third-order nonlinear polarization.

Finally, the state of the system is probed at $t=t_1$ through its dipole moment. The third-order response functions [Eqs. (2.7) and (2.9)] can also be read accordingly.

Many analyses of 2D-IR responses are based on the stochastic approach, which has been extensively used in electronically resonant spectroscopy.[1,39] This theory assumes that the bath induces Gaussian stochastic fluctuation $\hbar\delta\omega_v(t)$ on the energy levels of the oscillator mode and replaces the total Hamiltonian with *neglecting any dissipation* by the effective Hamiltonian,

$$\hat{H}_{\text{tot}}(t) = \sum_{v=0}^{v_{\max}} \hbar[\omega_v + \delta\omega_v(t)]|v\rangle\langle v|. \qquad (2.10)$$

For intramolecular vibrational modes satisfying $\beta\hbar\omega_{10}/2 \gtrsim 1$, we can derive the expressions for the rephasing and nonrephasing response functions as[1,37]

$$
\begin{aligned}
R_I^{(3)}(t_3, t_2, t_1) &\simeq \left(\frac{i}{\hbar}\right)^3 e^{-i\omega_{10}(t_3-t_1)} \times e^{-g(t_3)-g(t_1)+f(t_3,t_2,t_1)} \\
&\times (2\mu_{10}^4 - \mu_{10}^2\mu_{21}^2 e^{i\Delta_{\text{anh}}t_3})
\end{aligned} \quad (2.11a)
$$

and

$$
\begin{aligned}
R_{II}^{(3)}(t_3, t_2, t_1) &\simeq \left(\frac{i}{\hbar}\right)^3 e^{-i\omega_{10}(t_3+t_1)} \times e^{-g(t_3)-g(t_1)-f(t_3,t_2,t_1)} \\
&\times (2\mu_{10}^4 - \mu_{10}^2\mu_{21}^2 e^{i\Delta_{\text{anh}}t_3}),
\end{aligned} \quad (2.11b)
$$

respectively. Here, $g(t)$ is the line shape function defined as

$$g(t) \equiv \int_0^t d\tau \int_0^{\tau} d\tau'\, C_{\omega\omega}(\tau') \qquad (2.12)$$

for the classical time correlation function of the vibrational frequency,

$$C_{\omega\omega}(t) \equiv \langle \delta\omega_{10}(t)\delta\omega_{10}(0)\rangle_0, \qquad (2.13)$$

and $f(t_3,t_2,t_1)$ is the auxiliary function given by

$$f(t_3,t_2,t_1) \equiv g(t_2) - g(t_2+t_1) - g(t_3+t_2) + g(t_3+t_2+t_1). \qquad (2.14)$$

Due to this handiness, the stochastic approach has been employed to study not only the electronic dephasing but also vibrational dephasing. We should notice that the above-mentioned formalism involves only frequency fluctuation without any accounts of excited energy relaxation. In contrast with the electronic case, the vibrational modes in molecules strongly coupled to the bath modes that often relax excitation energy on a time scale comparable with the vibrational dephasing. In addition, as we will show in Sec. IV, if the mode is anharmonic, the energy relaxation process also induces vibrational dephasing, which may not be separated from the other dephasing effects. The interplay between the energy relaxation and dephasing is also nontrivial. To take into account the effect of energy relaxation, one often employs a simple Bloch picture. However, it is an open question that the phenomenological treatment of energy dissipation is valid, because the Bloch picture assumes a white noise bath and a weak system-bath coupling with the RWA. Such treatment cannot overcome the difficulty inherent in the stochastic approach; the stochastic theory itself does not account for the dissipation and temperature effects, both of which cause the energy relaxation toward the thermal equilibrium state. Generally, the dissipation relaxes the system to a "dead" state, while the fluctuation keeps the system "alive."[77] The balance between the fluctuation and dissipation is required to have a thermal equilibrium state at long times (fluctuation-dissipation theorem). Hence, the stochastic theory without indwelling the dissipation corresponds to the unphysical picture where the fluctuation continues to activate the system toward the infinite temperature.[39]

Experimental studies have indicated that the correlation function of $\delta\omega_{10}(t)$ decays on (at least) two time scales,[37] an ultrafast component on a several tens of femtoseconds time scale and a slower diffusion-controlled component. The ultrafast component is typically discussed in the motional narrowing limit. Then, Eq. (2.13) is assumed to be a sum of (at least) two exponentials. In order to focus on the validity of the employed stochastic model for the intramolecular vibrations, hereafter, we assume that the fluctuation $\delta\omega_{10}(t)$ can be described as a Markovian process, that is, Eq. (2.13) is a single exponential decay form (Anderson-Kubo process):

$$C_{\omega\omega}(t) = \Delta^2 e^{-\gamma t}, \qquad (2.15)$$

where Δ is the root-mean-squared amplitude of the fluctuation $\delta\omega_{10}(t)$ and γ^{-1} is their correlation time. The line shape function $g(t)$ is then be expressed as

$$g(t) = \frac{\Delta^2}{\gamma^2}(\gamma t + e^{-\gamma t} - 1). \qquad (2.16)$$

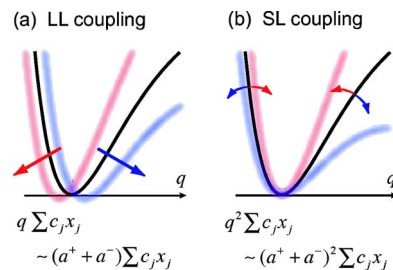We will use the above expression to obtain optical signals for stochastic cases.

FIG. 2. Schematic illustrations of effects of (a) the linear-linear (LL) and (b) the square-linear (SL) system-bath couplings on an anharmonic potential. The black lines represent the unperturbed potential, while the colored lines the perturbed ones. LL coupling swings the position of the potential minimum and deforms the potential, whereas SL coupling alters the curvature of the potential. Hence, both couplings induce the frequency fluctuation. Note that the LL and SL couplings mainly cause the one- and two-quantum transitions, respectively, as can be seen from the system-bath coupling expressed by the one-quantum creation and annihilation operators $\hat{a}^+$ and $\hat{a}^-$.

III. ANHARMONIC OSCILLATOR NONLINEARLY COUPLED TO HEAT BATH: REDUCED EQUATION OF MOTION APPROACH

To remedy the drawback of the stochastic theory mentioned in Sec. II, we consider an oscillator nonlinearly coupled to a heat bath composed of harmonic oscillators. The total Hamiltonian is expressed as

$$\hat{H}_{tot} = \hat{H} + \sum_j \left[\frac{\hat{p}_j^2}{2m_j} + \frac{m_j\omega_j^2}{2}\left(\hat{x}_j - \frac{c_j V(\hat{q})}{m_j\omega_j^2}\right)^2 \right], \qquad (3.1)$$

where the parameters $\hat{x}_j$, $\hat{p}_j$, m_j, and ω_j are the coordinate, momentum, mass, and frequency of the jth bath oscillator, respectively. In Eq. (3.1), the system-bath interaction is expressed as $F(\hat{q},\{x_j\}) = V(\hat{q})\Sigma_j c_j \hat{x}_j$, where $V(\hat{q})$ is a function whose dimension is the same as $\hat{q}$. We have included the counterterm $\Sigma_j c_j^2 V(\hat{q})^2/2m_j\omega_j^2$ in Eq. (3.1) to maintain the translational symmetry of the Hamiltonian for $U(\hat{q})=0$.[39,78] We expand $V(\hat{q})$ up to the second order in $\hat{q}$ as follows:

$$V(\hat{q}) = \frac{v_{LL}}{1!}\hat{q} + \frac{v_{SL}}{2!}\hat{q}^2. \qquad (3.2)$$

In Eq. (3.1), we refer to the terms proportional to v_{LL} and v_{SL} as the linear-linear (LL) and square-linear (SL) couplings, respectively. For anharmonic vibrational modes, the LL coupling term deforms the potential curve and induces frequency fluctuation.[79,80] The SL coupling[10,11,81,82] mainly modulates the curvature of $U(q)$ in accordance with the time evolution of $\{x_j\}$. Hence, the frequency in the present model fluctuates on a time scale of bath dynamics based on two distinct scenarios (see Fig. 2).

The character of bath is specified by the spectral distribution function $J(\omega) \equiv \Sigma_j[c_j^2/(2m_j\omega_j)]\delta(\omega-\omega_j)$. We consider the nearly Gaussian-Markovian noise bath, whose distribution function is given by the Ohmic form with the Lorentzian cutoff:[83]

$$J(\omega) = \frac{m\zeta}{\pi}\frac{\gamma^2}{\omega^2+\gamma^2}\omega, \qquad (3.3)$$

where γ represents the width of the spectral distribution of the bath modes and is related to the correlation time of the

noise induced by the bath: $\tau = \gamma^{-1}$. This can be seen from the symmetrized correlation function of the collective bath coordinate,

$$\hat{X} \equiv \sum_j c_j \hat{x}_j. \tag{3.4}$$

Within the condition of $\beta\hbar\gamma/2 \lesssim 1$, we have[39]

$$\frac{1}{2}\langle \hat{X}(t)\hat{X}(0) + \hat{X}(0)\hat{X}(t)\rangle_b \simeq \frac{m}{\beta}\zeta\gamma e^{-\gamma t}, \tag{3.5}$$

where $\hat{X}(t)$ is the Heisenberg representation of $\hat{X}$ and $\langle\cdots\rangle_b$ is the canonical thermal average with respect to the bath degrees of freedom. This indicates that the bath oscillators disturb the system with the Gaussian-Markovian noise. Using some characteristic frequency of the system ω_c, we introduce the dimensionless coordinate $\hat{Q} \equiv \hat{q}\sqrt{m\omega_c/\hbar}$ and coefficients

$V_{LL} \equiv v_{LL}$ and $V_{SL} \equiv v_{SL}\sqrt{\hbar/m\omega_c}$ and rewrite Eq. (3.2) as

$$V(\hat{q}) = \sqrt{\frac{\hbar}{m\omega_c}}\left(V_{LL}\hat{Q} + \frac{V_{SL}}{2}\hat{Q}^2\right) \equiv \sqrt{\frac{\hbar}{m\omega_c}}\mathcal{V}(\hat{Q}). \tag{3.6}$$

Here, we define the LL and SL coupling strengths by

$$\zeta_{LL} = V_{LL}^2\zeta, \quad \zeta_{SL} = V_{SL}^2\zeta, \tag{3.7}$$

respectively. Thus the effects of the system-bath interaction can be characterized by a set of four parameters β, ζ_{LL}, ζ_{SL}, and γ for ω_c.

The reduced description of the system can be introduced by tracing over the optically inactive bath degrees of freedom denoted by $\{x_j\}$ from the total density operator.[78,84,85] As shown in Ref. 76, dynamics of the reduced density operator for the system equation (3.1) with Eq. (3.3) is described by the LTC-QFP equation expressed as

$$\frac{\partial}{\partial t}\hat{\rho}_{j_1,\ldots,j_K}^{(n)}(t) = -\left[i\hat{\mathcal{L}} + n\gamma + \sum_{k=1}^{K}(j_k\nu_k + \hat{\Phi}\hat{\Psi}_k) + \hat{\Xi}\right]\hat{\rho}_{j_1,\ldots,j_K}^{(n)}(t) - \hat{\Phi}\hat{\rho}_{j_1,\ldots,j_K}^{(n+1)}(t) - n\gamma\hat{\Theta}\hat{\rho}_{j_1,\ldots,j_K}^{(n-1)}(t)$$
$$- \sum_{k=1}^{K}\hat{\Phi}\hat{\rho}_{j_1,\ldots,j_k+1,\ldots,j_K}^{(n)}(t) - \sum_{k=1}^{K}j_k\nu_k\hat{\Psi}_k\hat{\rho}_{j_1,\ldots,j_k-1,\ldots,j_K}^{(n)}(t) \tag{3.8}$$

for non-negative integers $n, j_1, \ldots, j_K$, where we determine the value of K so as to satisfy

$$\nu_K \gg \omega_c, \tag{3.9}$$

for bosonic Matsubara frequencies $\nu_k = 2\pi k/(\beta\hbar)$. In Eq. (3.8), $i\hat{\mathcal{L}} \equiv (i/\hbar)\hat{H}^\times$ is the quantal Liouvillian of the system and $\hat{\Phi}$, $\hat{\Theta}$, $\hat{\Psi}_k$, and $\hat{\Xi}$ are the bath-induced relaxation operators defined by

$$\hat{\Phi} \equiv \frac{i}{\hbar}V^\times(\hat{q}), \tag{3.10a}$$

$$\hat{\Theta} \equiv i\frac{m\zeta}{\beta\hbar}\left[-i\frac{\beta\hbar\gamma}{2}V^\circ(\hat{q}) + \frac{\beta\hbar\gamma}{2}\cot\left(\frac{\beta\hbar\gamma}{2}\right)V^\times(\hat{q})\right], \tag{3.10b}$$

$$\hat{\Psi}_k \equiv i\frac{m\zeta}{\beta\hbar}\frac{2\gamma^2}{\nu_k^2 - \gamma^2}V^\times(\hat{q}), \tag{3.10c}$$

and

$$\hat{\Xi} \equiv \frac{m\zeta}{\beta\hbar^2}\left[1 - \frac{\beta\hbar\gamma}{2}\cot\left(\frac{\beta\hbar\gamma}{2}\right)\right]V^\times(\hat{q})V^\times(\hat{q})$$
$$+ i\frac{m\zeta}{\beta\hbar^2}\frac{\beta\hbar\gamma}{2}V^\circ(\hat{q})V^\times(\hat{q}). \tag{3.10d}$$

In Eq. (3.10d), the second term is derived from the counterterm mentioned above. Note that only $\hat{\rho}_{0,\ldots,0}^{(0)}(t) = \hat{\rho}(t)$ has a physical meaning, and the other elements $\hat{\rho}_{j_1,\ldots,j_K}^{(n)}$ for $(n; j_1, \ldots, j_K) \neq (0; 0, \ldots, 0)$ are the auxiliary operators being introduced for computational purposes only; the expression of $\rho_{j_1,\ldots,j_K}^{(n)}(t)$ is given by the Appendix. The $K+1$ dimensional hierarchy equations given by Eq. (3.8) continue to infinity, which is not easy to solve numerically. To terminate Eq. (3.8) at finite stages, we solve Eq. (3.8) formally as

$$\hat{\rho}_{j_1,\ldots,j_K}^{(n)}(t) = \int_{t_i}^{t}ds\, e^{-[i\hat{\mathcal{L}} + n\gamma + \sum_{k=1}^{K}(j_k\nu_k + \hat{\Phi}\hat{\Psi}_k) + \hat{\Xi}](t-s)}\left[-\hat{\Phi}\hat{\rho}_{j_1,\ldots,j_K}^{(n+1)}(s) - n\gamma\hat{\Theta}\hat{\rho}_{j_1,\ldots,j_K}^{(n-1)}(s)\right.$$
$$\left. - \sum_{k=1}^{K}\hat{\Phi}\hat{\rho}_{j_1,\ldots,j_k+1,\ldots,j_K}^{(n)}(s) - \sum_{k=1}^{K}j_k\nu_k\hat{\Psi}_k\hat{\rho}_{j_1,\ldots,j_k-1,\ldots,j_K}^{(n)}(s)\right]. \tag{3.11}$$

If $n\gamma + \Sigma_{k=1}^{K} j_k \nu_k$ is large enough compared with ω_c, the kernel of time integral can be replaced by Dirac's delta function as

$$\left(n\gamma + \sum_{k=1}^{K} j_k \nu_k \right) e^{-(n\gamma + \Sigma_{k=1}^{K} j_k \nu_k)(t-s)} \simeq \delta(t-s), \qquad (3.12)$$

and then Eq. (3.8) becomes

$$\frac{\partial}{\partial t} \hat{\rho}_{j_1,\dots,j_K}^{(n)}(t) \simeq -\left(i\hat{\mathcal{L}} + \sum_{k=1}^{K} \hat{\Phi}\hat{\Psi}_k + \hat{\Xi} \right) \hat{\rho}_{j_1,\dots,j_K}^{(n)}(t), \quad (3.13)$$

which works as the terminator for Eq. (3.8). This termination is valid for the integers $n, j_1, \dots, j_K$, satisfying

$$N \equiv n + \sum_{k=1}^{K} j_k \gg \frac{\omega_c}{\min(\gamma, \nu_1)}, \qquad (3.14)$$

because $n\gamma + \Sigma_{k=1}^{K} j_k \nu_k \gg (n + \Sigma_{k=1}^{K} j_k)\min(\gamma, \nu_1)$. This termination is simple and easy to utilize in numerical calculations. In practice, as demonstrated numerically in Ref. 76, we may use the lower values of K and N which do not satisfy Eqs. (3.9) and (3.14), respectively. This formalism has applicability to a low-temperature system $(\beta\omega_c/2 \gg 1)$ strongly coupled to the heat bath without employing RWA for the system-bath interaction. Namely, Eq. (3.8) with Eqs. (3.10) and (3.13) is free from the positivity problem,[86] where the populations of the excited states calculated from the reduced equations of motion such as the quantum master equation and the Redfield equation without RWA become negative at low temperatures. The advantage of Eq. (3.8) deserves explicit emphasis.

To calculate the optical responses [Eqs. (2.6) and (2.7)] from the equation of motion approach, we adapt the procedure presented in Ref. 39. We first have to generate the initial equilibrium state by integrating the equations of motion, Eqs. (3.8) and (3.13), until all hierarchical elements attain steady-state values. To have the equilibrium state, we set a temporally initial condition for the integration by

$$\hat{\rho}_{0,\dots,0}^{(0)}(t=t_i) = \frac{\exp(-\beta\hat{H})}{\mathrm{Tr}\exp(-\beta\hat{H})} \equiv \hat{\rho}^{\langle \mathrm{can}\rangle}, \qquad (3.15)$$

and $\hat{\rho}_{j_1,\dots,j_K}^{(n)}(t=t_i)=0$ for $(n;j_1,\dots,j_K)\neq(0;0,\dots,0)$. The generated initial state is then modified by the first laser pulse via the dipole operator as $(i/\hbar)\mu(\hat{q})^{\times}\hat{\rho}_{\mathrm{tot}}^{\mathrm{eq}}$. The perturbed density operator then evolves in time for the t_1 period following the equations of motion [Eqs. (3.8) and (3.13)]. First-order IR response function, Eq. (2.4), is then obtained by calculating the trace of $\mu(\hat{q})$. The third-order IR response functions [Eqs. (2.7) and (2.9)] can also be calculated in a similar manner.

The connection between the present approach and the stochastic approach can be seen as follows. When the temperature effects and vibrational energy relaxation are ignored, the LTC-QFP equation [Eq. (3.8)] reduces to

$$\frac{\partial}{\partial t}\hat{\rho}^{(n)}(t) = -(i\hat{\mathcal{L}} + n\gamma)\hat{\rho}^{(n)}(t) - \frac{i}{\hbar}\hat{W}^{\times}\hat{\rho}^{(n+1)}(t)$$

$$- in\frac{m\zeta\gamma}{\beta\hbar}\hat{W}^{\times}\hat{\rho}^{(n-1)}(t), \qquad (3.16)$$

where $\hat{W}$ is the adiabatic component of $V(\hat{q})$ defined by

$$\hat{W} \equiv \sum_v |v\rangle\langle v|V(\hat{q})|v\rangle\langle v|. \qquad (3.17)$$

Equation (3.16) is the extension of the stochastic Liouville equation[38,39] to a potential system (see Fig. 6). The comparison between Eq. (3.16) and the original stochastic Liouville equation tells us that the amplitude of the fluctuation $\delta\omega_{10}(t)$ is expressed as

$$\Delta = \mathrm{abs}\left[\mathrm{Tr}\{\hat{W}^{\times}|1\rangle\langle 0|\}\sqrt{\frac{m\zeta\gamma}{\beta\hbar^2}} \right] \qquad (3.18a)$$

$$= \mathrm{abs}\left[\mathrm{sgn}\left(\frac{\zeta_{\mathrm{LL}}}{\zeta_{\mathrm{SL}}}\right)(Q_{11}-Q_{00})\sqrt{\frac{\zeta_{\mathrm{LL}}\gamma}{\beta\hbar\omega_c}} \right.$$

$$\left. + \frac{1}{2}(Q_{11}^2 - Q_{00}^2)\sqrt{\frac{\zeta_{\mathrm{SL}}\gamma}{\beta\hbar\omega_c}} \right]. \qquad (3.18b)$$

From Eq. (3.18), we can estimate the amplitude of the frequency fluctuation in the system in accordance with the LTC-QFP [Eq. (3.8)].

IV. 2D-IR SPECTRA FOR MORSE SYSTEM WITH LL+SL COUPLING

We present the numerical results for Morse potential defined by

$$U(\hat{q}) = D_e(1 - e^{-\alpha\hat{q}})^2, \qquad (4.1)$$

where D_e denotes the dissociation energy. The vth eigenenergy for the Hamiltonian with the potential Eq. (4.1) is expressed as

$$\hbar\omega_v = \hbar\omega_c\left[\left(v + \frac{1}{2}\right) - \frac{\hbar}{2m\omega_c}\alpha^2\left(v + \frac{1}{2}\right)^2 \right], \qquad (4.2)$$

where $\omega_c = \sqrt{2D_e\alpha^2/m}$. Then, the anharmonicity $\Delta_{\mathrm{anh}} \equiv \omega_{10} - \omega_{21}$ and the fundamental frequency ω_{10} are given by $\Delta_{\mathrm{anh}} = \hbar\alpha^2/m$ and $\omega_{10} = \omega_c - \Delta_{\mathrm{anh}}$, respectively. The fundamental frequency and the anharmonicity of the system are set to be $\omega_{10} = 1600$ cm^{-1} $(2\pi/\omega_{10} = 20.8$ fs) and $\Delta_{\mathrm{anh}} = 16$ cm^{-1} $(\Delta_{\mathrm{anh}}/\omega_{10} = 0.01)$, which are in the typical range for intramolecular vibrational motion. We consider a room temperature heat bath, $T = 300$ K $(\beta\hbar\omega_{10} = 7.67)$. To carry out calculations, we employ the lowest six energy eigenstates to represent the system. The fourth-order Runge-Kutta method is used to numerically integrate the equation of motion. The time step for the finite difference expression for $\partial\hat{\rho}_{j_1,\dots,j_K}^{(n)}/\partial t$ is $\delta t = (1/\times\omega_{10})0.01$. We chose the depth of the hierarchy and the number of the Matsubara frequencies $N = 3-25$ and

$K=1-4$, respectively. The accuracy of the calculations is checked by changing the number of the energy eigenstates and the values of δt, N, and K. The dipole moment is assumed to be $\mu(\hat{q})=\mu_1\hat{q}$, and we set $\mu_1=1$ to calculate the 2D-IR signals. Under these conditions, we calculate 2D-IR correlation spectrum[87] defined as

$$S_C(\omega_3,\omega_1;t_2) \equiv S_R(\omega_3,-\omega_1;t_2) + S_{NR}(\omega_3,\omega_1;t_2), \quad (4.3)$$

where

$$S_R(\omega_3,\omega_1;t_2) \equiv \mathrm{Im} \int_0^\infty dt_3 e^{i\omega_3 t_3} \int_0^\infty dt_1 e^{i\omega_1 t_1} R_I^{(3)}(t_3,t_2,t_1) \quad (4.4)$$

is 2D rephasing spectrum and

$$S_{NR}(\omega_3,\omega_1;t_2) \equiv \mathrm{Im} \int_0^\infty dt_3 e^{i\omega_3 t_3} \int_0^\infty dt_1 e^{i\omega_1 t_1} R_{II}^{(3)}(t_3,t_2,t_1) \quad (4.5)$$

is 2D nonrephasing spectrum.

A. Motional narrowing regime

Figure 3 presents 2D-IR correlation spectra $S_C(\omega_3,\omega_1;t_2=0)$ for $\gamma/\omega_{10}=0.5$ ($\gamma^{-1}=6.6$ fs). In the figure, the panels (a) are calculated by integrating the LTC-QFP equation, Eq. (3.8), while the panels (b) by the stochastic model, Eq. (2.11). The system-bath coupling $(\zeta_{LL},\zeta_{SL})/\omega_{10}$ for panels (a) are chosen to be (i) $(+0.05,0)$, (ii) $(0,+0.05)$, (iii) $(+0.05,+0.05)$, and (iv) $(-0.05,+0.05)$, respectively. The parameters for the stochastic case shown in (b) are evaluated from those in (a) using Eq. (3.18) and the values of Q_{vv} and Q_{vv}^2; for the present system, we have $Q_{00}=0.074$, $Q_{11}=0.226$, $Q_{00}^2=0.509$, and $Q_{11}^2=1.567$. The amplitude of frequency fluctuation Δ for each panel are calculated as (i) 13.7 cm^{-1} ($\Delta/\gamma=0.01$), (ii) 48.1 cm^{-1} ($\Delta/\gamma=0.06$), (iii) 61.8 cm^{-1} ($\Delta/\gamma=0.08$), and (iv) 34.3 cm^{-1} ($\Delta/\gamma=0.04$). As seen from the gradient of the 2D line shapes, these are in the motional narrowing regime without the inhomogeneity.

In this large γ case, the spectra calculated by the LTC-QFP equation are quite different from the stochastic results due to energy relaxation missing in the stochastic approach. The linewidth of the spectra from the stochastic approach (b-i) is very small in this motional narrowing regime, whereas the spectra from the LTC-QFP equation case (a-i) are broad because vibrational dephasing is dominated by energy relaxation rather than elastic pure dephasing.

We now consider the SL coupling case [(a-ii) and (b-ii)]. As mentioned in Fig. 2, the SL coupling term, $\hat{q}^2\Sigma_j c_j\hat{x}_j$, mainly induces the two-quantum transition as well as the curvature modulation of the potential. The population relaxations $1\rightarrow0$ and $2\rightarrow1$ are *almost* prohibited, whereas the relaxation $2\rightarrow0$ is allowed. (The one-quantum relaxations are not *completely* prohibited because of the anharmonicity of potential.) As a result, energy relaxation destroys only the
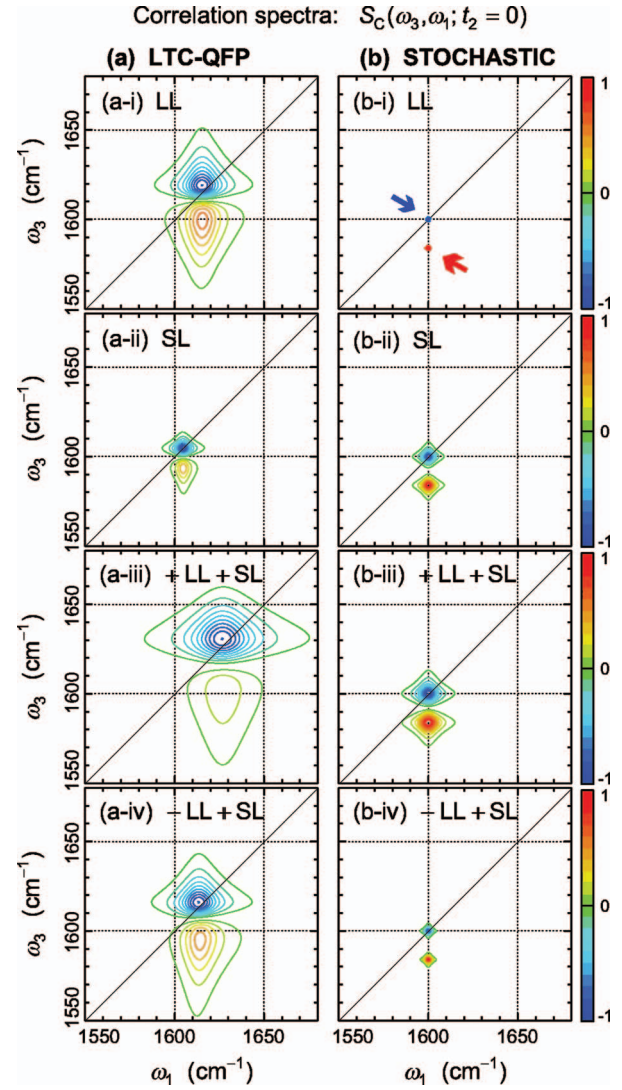

FIG. 3. (Color) 2D-IR correlation spectra $S_C(\omega_3,\omega_1;t_2=0)$ of the Morse oscillator ($\omega_{10}=1600$ cm^{-1}, $\Delta_{anh}=16$ cm^{-1}) in the *motional narrowing* regime. The spectra were calculated from (a) the LTC-QFP approach with Eq. (3.8) and (b) the stochastic approach with Eq. (2.11) with the coupling strength and the amplitude of fluctuation adjusted by Eq. (3.18). The panels from the top to bottom show the signals for (i) LL, (ii) SL, (iii) +LL+SL, and (iv) −LL+SL system-bath coupling cases, respectively. The noise correlation time is in the motional narrowing regime ($\gamma^{-1}=6.6$ fs). The negative-going peaks arise from the 0-1 transition, whereas the positive-going peaks from the 1-2 transition.

1–2 coherence. Hence, the positive-going peaks (1–2 transition) in the two panels are different, while the negative-going peaks (0–1 transition) have similar characteristics.

Next, we discuss the difference between the +LL+SL and −LL+SL coupling cases. As is evident from Eq. (3.18), the +LL+SL coupling reinforces the amplitude of frequency fluctuation, while the −LL+SL coupling diminishes the amplitude. The amplitude of fluctuation affects the strength of pure dephasing in the stochastic case. Therefore the line shapes from the stochastic approach [(b-iii) and (b-iv)] are different. The primary relaxation processes in the LTC-QFP equation case shown in (a-iii) and (a-iv) are, however, energy relaxation rather than pure dephasing; therefore, the profiles in (a-iii) and (a-iv) are also different from those in (b-iii) and (b-iv). The difference between (a-iii) and (a-iv) is caused

from the cross term contribution between the LL and SL couplings.[18,82] To explain this, we consider the classical generalized Langevin equation (GLE) for the Hamiltonian equation (3.1),[74]

$$m\ddot{q}_t = -U'(q_t) - m\int_0^t ds \underbrace{V'(q_t)\eta(t-s)V'(q_s)}_{\text{dissipation}:\Gamma(t-s)}\dot{q}_s + \underbrace{V'(q_t)\xi(t)}_{\text{fluctuation}},$$

(4.6)

where the fluctuation $\xi(t)$ and the dissipation $\eta(t)$ are related by the fluctuation-dissipation theorem $\langle\xi(t)\xi(s)\rangle_0 = m \times \eta(t-s)/\beta$, in which $\langle\cdots\rangle_0$ denotes the statistical average. For $+$LL$+$SL coupling $V(q)=+v_{LL}q+v_{SL}q^2/2$, the integral kernel $\Gamma(t-s)=V'(q_t)\eta(t-s)V'(q_s)$ in Eq. (4.6) is expressed as

$$\Gamma(t-s) = \left[v_{LL}^2 + \frac{v_{SL}^2}{4}q_t q_s\right]\eta(t-s) + \frac{v_{LL}v_{SL}}{2}[q_t+q_s]\eta(t-s),$$

(4.7)

whereas for $-$LL$+$SL coupling $V(q)=-v_{LL}+v_{SL}q^2/2$, $\Gamma(t-s)$ is given by

$$\Gamma(t-s) = \left[v_{LL}^2 + \frac{v_{SL}^2}{4}q_t q_s\right]\eta(t-s) - \frac{v_{LL}v_{SL}}{2}[q_t+q_s]\eta(t-s).$$

(4.8)

The difference between Eqs. (4.7) and (4.8) is on the sign of the term proportional to $v_{LL}v_{SL}$; the difference between the panels (a-iii) and (a-iv) arises only from the cross term contribution between the LL and SL couplings.

In the stochastic case (b), the negative-going peaks (0–1 coherence) and the positive-going peaks (1–2 coherence) are located on $(\omega_1,\omega_3)=(\omega_{10},\omega_{10})$ and $(\omega_{10},\omega_{10}-\Delta_{anh})$, respectively. In the LTC-QFP equation case (a), however, we can see that the spectral peak locations shift toward the upper right. These 2D blueshifts arise purely from the dissipation with the finite noise correlation time. To illustrate this, we consider a harmonic potential $U(q)=m\omega_{10}^2 q^2/2$ in the presence of only the LL coupling $V(q)=q$ with the Markovian noise bath $\eta(t)=\zeta\gamma e^{-\gamma t}$ and depict linear absorption spectra. The analytic expression of the absorption spectrum (first-order response) for this system is obtained as

$$I(\omega) \equiv \text{Im}\int_0^\infty dt e^{i\omega t}\left[-\beta\frac{d}{dt}\langle q(t)q(0)\rangle_0\right]$$

(4.9a)

$$= \frac{\omega_{10}^2\langle q(0)^2\rangle_0\beta\zeta\omega}{(\omega^2-\omega_{10}^2)^2 + \zeta^2\omega^2 G_\gamma(\omega)},$$

(4.9b)

with

$$G_\gamma(\omega) \equiv \left(\frac{\omega^2-\omega_{10}^2}{\zeta\gamma}-1\right)^2.$$

(4.9c)

If $\gamma\to\infty$, the result reduces to the white noise case with $G_\gamma(\omega)\to1$. We show the linear absorption spectra calculated for Markovian noise and white noise cases in Fig. 4. Here, we set $\gamma/\omega_{10}=0.5$ and $\zeta/\omega_{10}=0.05$, which are the same values as in Fig. 3. As clearly seen from the figure, the dissipa-
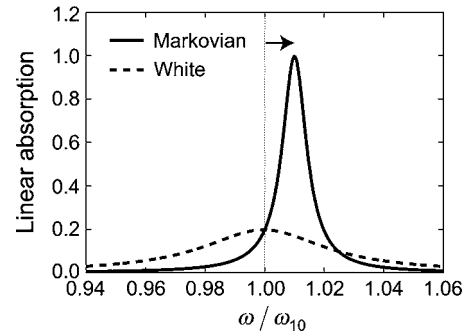

FIG. 4. Linear absorption spectra calculated from Eq. (4.9) for the Markovian noise case ($\gamma=0.5\omega_{10}$) and the white noise case ($\gamma\to\infty$). We set the system-bath coupling strength for both to $\zeta=0.05\omega_{10}$. The normalization of each spectrum is such that the maximum of the spectrum for the Markovian case is unity.

tion with the finite noise correlation time causes the blueshift of the spectral peak position. We cannot obtain such analytic expression for the SL coupling case as Eq. (4.9b). Notice, however, that the SL coupling induces the dissipation involving two-quantum relaxation, and then causes the blueshift. Since characters of 2D-IR spectra and linear absorption are both determined from the time propagator as illustrated in Eqs. (2.7) and (2.6), the spectral peaks in 2D-IR spectra also exhibit the blueshifts.

B. Spectral diffusion regime

Figure 5 presents 2D-IR correlation spectra $S_C(\omega_3,\omega_1;t_2=0)$ for small γ. In the figure, the panels (a) are calculated by integrating the LTC-QFP equation [Eq. (3.8)], while the panels (b) by the stochastic result [Eq. (2.11)]. The inverse noise correlation time is set to be $\gamma/\omega_{10}=0.005$ ($\gamma^{-1}=0.66$ ps). The system-bath coupling strengths $(\zeta_{LL},\zeta_{SL})/\omega_{10}$ for panels (a) are chosen to be (i) $(+2,0)$, (ii) $(0,+0.5)$, (iii) $(+2,+0.5)$, and (iv) $(-2,+0.5)$, respectively. As in the motional narrowing cases, we can evaluate the amplitude of frequency fluctuation Δ for (b) as follows: (i) 8.7 cm^{-1} ($\Delta/\gamma=1.1$), (ii) 15.2 cm^{-1} ($\Delta/\gamma=1.9$), (iii) 23.9 cm^{-1} ($\Delta/\gamma=3.0$), and (iv) 6.5 cm^{-1} ($\Delta/\gamma=0.8$). As seen from the profiles of the 2D line shapes, these are in the spectral diffusion regime with moderate inhomogeneity.

In this small γ case, the spectra calculated by the LTC-QFP equation resemble those from the stochastic approach. This similarity indicates that vibrational dephasing processes in the present situation are dominated by elastic pure dephasing rather than by energy relaxation; hence, the stochastic theory is a good description for 2D line shapes. However, compared with the cases in (b), the peak positions for the LTC-QFP equation case in (a) slightly shift toward the upper right. The cause of the blueshifts is the dissipation with finite noise correlation time, as mentioned in Sec. IV A. This fact indicates that although the effect of vibrational energy relaxation in comparison to that of frequency fluctuation process is small, still there exist effects of dissipation caused by the system-bath coupling. The stochastic theory, which neglects any dissipation, cannot explain the 2D blueshifts.
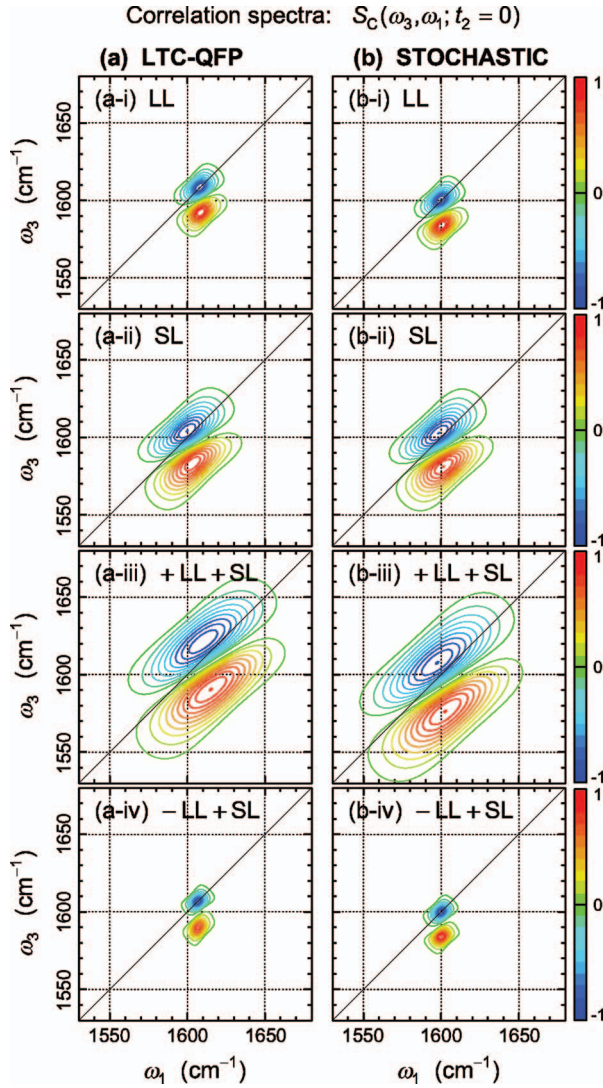
FIG. 5. (Color) 2D-IR correlation spectra $S_C(\omega_3, \omega_1; t_2=0)$ of the Morse oscillator ($\omega_{10}=1600$ cm^{-1}, $\Delta_{anh}=16$ cm^{-1}) in the *spectral diffusion* regime. The spectra were calculated from (a) the LTC-QFP approach with Eq. (3.8) and (b) the stochastic approach with Eq. (2.11). The panels from the top to bottom show the spectra for (i) LL, (ii) SL, (iii) +LL+SL, and (iv) −LL +SL system-bath coupling cases, respectively. The inverse noise correlation time is $\gamma/\omega_{10}=0.005$ ($\gamma^{-1}=0.66$ ps). The negative-going peaks arise from the 0-1 transition, whereas the positive-going peaks from the 1-2 transition.

C. Preconditions of stochastic theory for vibrational dephasing

We now discuss the precondition of the the stochastic theory to apply molecular vibrational motion. First we should notice that the system can efficiently exchange energy quanta with the bath, if there are bath modes whose frequencies are similar to the characteristic frequency of the system ω_c. If $\gamma \ll \omega_c$, however, such bath modes are virtually nonexistent. If the condition $\gamma \gtrsim \omega_c$ is satisfied, the spectral distribution Eq. (3.3) reduces to $J(\omega_c) \simeq (m\zeta/\pi)\omega_c$, which suggests that there are plenty of bath modes which can efficiently exchange energy with the system oscillator. On the contrary, when the condition $\gamma \ll \omega_c$ holds, we have $J(\omega_c) \simeq (m\zeta/\pi)\omega_c(\gamma/\omega_c)^2 \approx 0$, which indicates that the system oscillator cannot readily exchange energy with the bath modes, and therefore the bath modes can barely contribute to the energy relaxation.

To estimate the strength of dissipation, we utilize the correlation function of the collective bath coordinate [Eq. (3.4)],

$$\langle \hat{X}(t)\hat{X}(0)\rangle_b \equiv \mathsf{C}'(t) + i\mathsf{C}''(t), \tag{4.10}$$

where $\mathsf{C}'(t)$ is the real part of $\langle \hat{X}(t)\hat{X}(0)\rangle_b$ that relates to fluctuation and $\mathsf{C}''(t)$ is the imaginary part that relates to dissipation.[39,83] For Eq. (3.3), they are expressed as

$$\mathsf{C}'(t) \simeq \frac{m}{\beta}\zeta\gamma e^{-\gamma t}, \tag{4.11}$$

$$\mathsf{C}''(t) = -\frac{\beta\hbar\gamma}{2}\frac{m}{\beta}\zeta\gamma e^{-\gamma t}, \tag{4.12}$$

where we assumed that $\beta\hbar\gamma/2 \ll 1$ in Eq. (4.11), and therefore we have

$$\left|\frac{\mathsf{C}''(t)}{\mathsf{C}'(t)}\right| \ll 1. \tag{4.13}$$

This indicates that the dissipation is negligible relative to the fluctuation for $\beta\hbar\gamma/2 \ll 1$.

Summarizing two conditions, we have

$$\gamma \ll \omega_c, \quad \beta\hbar\gamma/2 \ll 1. \tag{4.14}$$

As long as the above conditions are satisfied, the energy relaxation plays a minor role compared with the elastic pure dephasing, and the vibrational dephasing is dominated by the pure dephasing caused by the frequency fluctuation rather than the energy relaxation. In such cases, the stochastic theory may be applied to analyze 2D line shapes although the theory cannot account such dissipative effects as the blueshifts.

V. CONCLUDING REMARKS

In this paper, we considered an anharmonic potential system coupled to a colored noise bath with linear-linear (LL) and square-linear (SL) system-bath interactions. For the system, we introduced the low-temperature corrected quantum Fokker-Planck (LTC-QFP) equation, which can describe an anharmonic intramolecular vibration at temperature much lower than vibrational excitation energy (a low-temperature system). It is noteworthy that the equation is based on the vibrational coordinate and is not afflicted with the positivity problem that occurs in a low-temperature system without the rotating wave approximation, as opposed to the conventional quantum master equation or Bloch-Redfield equation. By utilizing the equation we calculated 2D-IR correlation spectra for various system-bath parameters. Our formalism, LTC-QFP equation, can treat a dissipation-dominant regime (Fig. 3) and a fluctuation-dominant regime (Fig. 5) in a unified framework. We found the profiles of 2D-IR spectra change dramatically with a form and strength of system-bath coupling and a noise correlation time. In this anharmonic system, the LL coupling leads to not only one-quantum relaxation but also the deformation of a potential curve, whereas the SL coupling gives rise to a curvature modulation of the potential curve in addition to two-quantum relaxation.
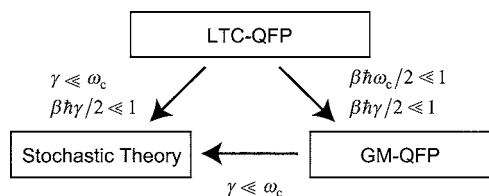
FIG. 6. Applicability of various approaches. The low-temperature corrected quantum Fokker-Planck (LTC-QFP) equation [Eq. (3.8)] reduces to the Gaussian-Markovian quantum Fokker-Planck (GM-QFP) equation at high temperature (Refs. 11, 39, 75, and 82). When the two conditions $\gamma \ll \omega_c$ and $\beta\hbar\gamma/2 \ll 1$ are satisfied simultaneously, the LTC-QFP and GM-QFP agree with the results from the stochastic theory besides the effects of blueshifts due to the dissipation with the finite noise correlation time.

Through 2D-IR spectra, we clarify the details of the system-bath coupling as follows: (1) the difference between one- and two-quantum relaxations, (2) a cross term contribution between the LL and SL couplings, and (3) the interplay between the LL and SL mechanisms of frequency fluctuation (Fig. 2).

We also discussed the precondition for validity of the stochastic approach. Since the stochastic theory breaks down for a system where the energy relaxation is significant because the theory neglects any dissipative effects, we focus on the case where energy dissipative effects can be ignored. Then we found that if the noise correlation time $\tau = \gamma^{-1}$ satisfies the following two conditions, (a) $\gamma \ll \omega_c$ for the characteristic frequency of the system oscillator ω_c and (b) $\beta\hbar\gamma/2 \ll 1$ for the inverse temperature β, we may disregard energy dissipation processes in comparison with dephasing processes (see Fig. 6). Within the two conditions, the stochastic theory can explain the line shapes of the multidimensional vibrational spectra, regardless of the characteristic frequency of the system such as $\beta\hbar\omega_c/2 \gg 1$ or $\beta\hbar\omega_c/2 \ll 1$), besides the blueshifts caused by the dissipation from colored noise bath.

In this paper, we restricted our discussions to a single anharmonic mode in a bath characterized by a single decay constant γ. Extension to multimodal anharmonic systems in more realistic bath is left for future studies.

ACKNOWLEDGMENTS

APPENDIX: DERIVATION OF LOW-TEMPERATURE CORRECTED QUANTUM FOKKER-PLANCK EQUATION

In this appendix, we outline a derivation of the quantal equation of motion for a reduced density matrix, which has applicability to a low-temperature system ($\beta\hbar\omega_c/2 \gg 1$) that can be used to analyze an intramolecular vibrational mode.[39,76]

The reduced density matrix element for the system is expressed in the path integral form with the factorized initial condition as

$$
\rho(q,q';t) = \int dq_i \int dq_i' \int \mathcal{D}q \int \mathcal{D}q' \exp\left[\frac{i}{\hbar}(S[q] - S[q'])\right] \mathcal{F}_{\mathrm{FV}}[q,q'] \rho(q_i,q_i';t_i). \tag{A1}
$$

Here, $S[q]$ is the action of the system and $\mathcal{F}_{\mathrm{FV}}[q,q']$ is the Feynman-Vernon influence functional given by[84]

$$
\mathcal{F}_{\mathrm{FV}}[q,q'] = \exp\left(-\frac{1}{\hbar}\int_0^\infty d\omega J(\omega)\int_{t_i}^t ds \int_{t_i}^s ds' V^\times(s) \right.
$$
$$
\times \left[V^\times(s')\coth\left(\frac{\beta\hbar\omega}{2}\right)\cos(\omega(s-s')) \right.
$$
$$
\left.\left. - iV^\circ(s')\sin(\omega(s-s')) \right]\right)
$$
$$
\times \exp\left(-\frac{i}{\hbar}\int_{t_i}^t ds[\Delta U(q_s) - \Delta U(q_s')]\right), \tag{A2}
$$

where we have introduced the abbreviations $V^\times(t) \equiv V(q_t) - V(q_t')$ and $V^\circ(t) \equiv V(q_t) + V(q_t')$. The counterterm $\Delta U(q) = \int_0^\infty d\omega J(\omega) V(q)^2/\omega$ found in Eq. (3.1) is taken into account as the second exponential on the right-hand side of Eq. (A2). For the distribution Eq. (3.3), we can rewrite Eq. (A2) as

$$
\mathcal{F}_{\mathrm{FV}}[q,q'] = \exp\left(\int_{t_i}^t ds \int_{t_i}^s ds' \Phi(s)\Theta(s)\gamma e^{-\gamma(s-s')}\right)
$$
$$
\times \prod_{k=1}^\infty \exp\left(\int_{t_i}^t ds \int_{t_i}^s ds' \Phi(s)\Psi_k(s')\nu_k e^{-\nu_k(s-s')}\right)
$$
$$
\times \exp\left(-\frac{i}{\hbar}\int_{t_i}^t ds \frac{m\zeta\gamma}{2}V^\circ(s)V^\times(s)\right), \tag{A3}
$$

with

$$
\Phi(t) \equiv \frac{i}{\hbar}V^\times(t), \tag{A4}
$$

$$
\Theta(t) \equiv i\frac{m\zeta}{\beta\hbar}\left[-i\frac{\beta\hbar\gamma}{2}V^\circ(t) + \frac{\beta\hbar\gamma}{2}\cot\left(\frac{\beta\hbar\gamma}{2}\right)V^\times(t)\right], \tag{A5}
$$

$$
\Psi_k(t) \equiv i\frac{m\zeta}{\beta\hbar}\frac{2\gamma^2}{\nu_k^2 - \gamma^2}V^\times(t), \tag{A6}
$$

where $\nu_k = 2\pi k/(\beta)$ is a bosonic Matsubara frequency.

If we choose K so as to satisfy $\nu_K \gg \omega_c$, the factor $e^{-\nu_k(s-s')}$ in Eq. (A3) can be replaced by Dirac's delta function as

$$
\nu_k e^{-\nu_k(s-s')} \simeq \delta(s-s') \quad (k \geq K+1). \tag{A7}
$$

Thus, by choosing the relevant K, Eq. (A3) can be reduced to

$$\mathcal{F}_{FV}[q,q'] \simeq \exp\left(-\int_{t_i}^t ds\,\Phi(s)e^{-\gamma s}\left[-\int_{t_i}^s ds'\,\gamma\Theta(s')e^{\gamma s'}\right]\right)$$

$$\times \prod_{k=1}^K \exp\left(-\int_{t_i}^t ds\,\Phi(s)e^{-\nu_k s}\left[-\int_{t_i}^s ds'\,\nu_k\Psi_k(s')e^{\nu_k s'}\right]\right)$$

$$\times \prod_{k=K+1}^\infty \exp\left(\int_{t_i}^t ds\,\Phi(s)\Psi_k(s)\right)\exp\left(-\frac{i}{\hbar}\int_{t_i}^t ds\,\frac{m\zeta\gamma}{2}V^\circ(s)V^\times(s)\right). \tag{A8}$$

In order to derive the equation of motion, we introduce the auxiliary operator $\hat{\rho}^{(n)}_{j_1,\ldots,j_K}(t)$ defined by its matrix element as

$$\rho^{(n)}_{j_1,\ldots,j_K}(q,q';t) = \int dq_i \int dq'_i \int \mathcal{D}q \int \mathcal{D}q' \left\{e^{-\gamma t}\left[-\int_{t_i}^t ds\,\gamma\Theta(s)e^{\gamma s}\right]\right\}^n$$

$$\times \prod_{k=1}^K \left\{e^{-\nu_k t}\left[-\int_{t_i}^t ds\,\nu_k\Psi_k(s)e^{\nu_k s}\right]\right\}^{j_k}\exp\left[\frac{i}{\hbar}(S[q]-S[q'])\right]\mathcal{F}_{FV}[q,q']\rho(q_i,q'_i;t_i) \tag{A9}$$

for non-negative integers $n, j_1, \ldots, j_k$. Note that only $\hat{\rho}^{(0)}_{0,\ldots,0}(t) = \hat{\rho}(t)$ has a physical meaning, and the other elements $\hat{\rho}^{(n)}_{j_1,\ldots,j_K}$ for $(n;j_1,\ldots,j_K) \neq (0;0,\ldots,0)$ are introduced for computational purposes only. The differentiation of $\rho^{(n)}_{j_1,\ldots,j_K}(q,q';t)$ with respect to t gives rise to the factors from the time differentiation of the left- and right-hand side actions and the influence functional. The terms with these factors constitute the hierarchy members of Eq. (A9) with different n and $\{j_k\}$. As a result, we obtain the hierarchy of equations, Eq. (3.8).

[1] S. Mukamel, *Principles of Nonlinear Optical Spectroscopy* (Oxford University Press, New York, 1995).
[2] Y. Tanimura and S. Mukamel, J. Chem. Phys. **99**, 9496 (1993).
[3] K. Okumura and Y. Tanimura, J. Chem. Phys. **106**, 1687 (1997).
[4] K. Okumura and Y. Tanimura, J. Chem. Phys. **107**, 2267 (1997).
[5] K. Okumura and Y. Tanimura, Chem. Phys. Lett. **278**, 175 (1997).
[6] Y. Tanimura, Chem. Phys. **233**, 217 (1998).
[7] K. Okumura, A. Tokmakoff, and Y. Tanimura, J. Chem. Phys. **111**, 492 (1999).
[8] S. Mukamel, A. Piryantinski, and V. Chernyak, Acc. Chem. Res. **32**, 145 (1999).
[9] S. Mukamel, Annu. Rev. Phys. Chem. **51**, 691 (2000).
[10] T. Steffen and Y. Tanimura, J. Phys. Soc. Jpn. **69**, 3115 (2000).
[11] Y. Tanimura and T. Steffen, J. Phys. Soc. Jpn. **69**, 4095 (2000).
[12] M. Khalil and A. Tokmakoff, Chem. Phys. **266**, 213 (2001).
[13] C. Scheurer, A. Piryatinski, and S. Mukamel, J. Am. Chem. Soc. **123**, 3114 (2001).
[14] R. A. Denny and D. R. Reichman, J. Chem. Phys. **116**, 1987 (2002).
[15] R. Venkatramani and S. Mukamel, J. Chem. Phys. **117**, 11089 (2002).
[16] Y. Suzuki and Y. Tanimura, J. Chem. Phys. **119**, 1650 (2003).
[17] O. Kühn and Y. Tanimura, J. Chem. Phys. **119**, 2155 (2003).
[18] T. Kato and Y. Tanimura, J. Chem. Phys. **120**, 260 (2004).
[19] A. Ishizaki and Y. Tanimura, J. Chem. Phys. **123**, 014503 (2005).
[20] H.-D. Kim and Y. Tanimura, J. Chem. Phys. **123**, 224310 (2005).
[21] A. Ma and R. M. Stratt, Phys. Rev. Lett. **85**, 1004 (2000).
[22] T. L. C. Jansen, J. G. Snijders, and K. Duppen, J. Chem. Phys. **114**, 10910 (2001).
[23] S. Saito and I. Ohmine, Phys. Rev. Lett. **88**, 207401 (2002).
[24] J. Cao, S. Yang, and J. Wu, J. Chem. Phys. **116**, 3760 (2002).
[25] Y. Nagata and Y. Tanimura, J. Chem. Phys. **124**, 024508 (2006).
[26] K. Tominaga and K. Yoshihara, Phys. Rev. Lett. **74**, 3061 (1995).
[27] T. Steffen and K. Duppen, Phys. Rev. Lett. **76**, 1224 (1996).
[28] A. Tokmakoff, M. J. Lang, D. S. Larsen, G. R. Fleming, V. Chernyak, and S. Mukamel, Phys. Rev. Lett. **79**, 2702 (1997).

[29] A. Tokmakoff and G. R. Fleming, J. Chem. Phys. **106**, 2569 (1997).
[30] M. Cho, D. A. Blank, J. Sung, K. Park, S. Hahn, and G. R. Fleming, J. Chem. Phys. **112**, 2082 (2000).
[31] K. Tominaga and K. Yoshihara, J. Chin. Chem. Soc. (Taipei) **47**, 631 (2000).
[32] O. Golonzka, N. Demirdöven, M. Khalil, and A. Tokmakoff, J. Chem. Phys. **113**, 9893 (2000).
[33] J. C. Kirkwood and A. C. Albrecht, J. Raman Spectrosc. **31**, 107 (2000).
[34] K. J. Kubarych, C. J. Milne, S. Lin, V. Astinov, and R. J. D. Miller, J. Chem. Phys. **116**, 2016 (2002).
[35] L. J. Kaufman, J. Y. Heo, L. D. Ziegler, and G. R. Fleming, Phys. Rev. Lett. **88**, 207402 (2002).
[36] M. D. Fayer, Annu. Rev. Phys. Chem. **52**, 315 (2001).
[37] P. Hamm, M. Lim, and R. M. Hochstrasser, Phys. Rev. Lett. **81**, 5326 (1998).
[38] R. Kubo, Adv. Chem. Phys. **15**, 101 (1969).
[39] Y. Tanimura, J. Phys. Soc. Jpn. **75**, 082001 (2006).
[40] P. Hamm, M. Lim, and R. M. Hochstrasser, J. Phys. Chem. B **102**, 6123 (1998).
[41] M. Lim, P. Hamm, and R. M. Hochstrasser, Proc. Natl. Acad. Sci. U.S.A. **95**, 15315 (1998).
[42] K. Ohta, H. Maekawa, S. Saito, and K. Tominaga, J. Phys. Chem. A **107**, 5643 (2003).
[43] H. Maekawa, K. Ohta, and K. Tominaga, Phys. Chem. Chem. Phys. **6**, 4074 (2004).
[44] K. F. Everitt and J. L. Skinner, Chem. Phys. **266**, 197 (2001).
[45] K. F. Everitt, E. Geva, and J. L. Skinner, J. Chem. Phys. **114**, 1326 (2001).
[46] A. Piryatinski, C. P. Lawrence, and J. L. Skinner, J. Chem. Phys. **118**, 9664 (2003).
[47] A. Piryatinski, C. P. Lawrence, and J. L. Skinner, J. Chem. Phys. **118**, 9672 (2003).
[48] M. L. Cowan, B. D. Bruner, N. Huse, J. R. Dwyer, B. Chugh, E. T. J. Nibbering, T. Elsaesser, and R. J. D. Miller, Nature (London) **434**, 199 (2005).
[49] M. C. Asplund, M. T. Zanni, and R. M. Hochstrasser, Proc. Natl. Acad. Sci. U.S.A. **97**, 8219 (2000).
[50] M. T. Zanni, M. C. Asplund, and R. M. Hochstrasser, J. Chem. Phys. **114**, 4579 (2001).
[51] O. Golonzka, M. Khalil, N. Demirdöven, and A. Tokmakoff, Phys. Rev. Lett. **86**, 2154 (2001).
[52] N.-H. Ge, M. T. Zanni, and R. M. Hochstrasser, J. Phys. Chem. A **106**, 962 (2002).
[53] S. Woutersen and P. Hamm, J. Phys. Chem. B **104**, 11316 (2000).
[54] S. Woutersen and P. Hamm, J. Chem. Phys. **115**, 7737 (2001).
[55] S. Woutersen, Y. Mu, G. Stock, and P. Hamm, Proc. Natl. Acad. Sci. U.S.A. **98**, 11254 (2001).
[56] S. Woutersen and P. Hamm, J. Phys.: Condens. Matter **14**, 1035 (2002).

[57] J. Bredenbeck, J. Helbing, R. Behrendt, C. Renner, L. Moroder, J. Wachtveitl, and P. Hamm, J. Phys. Chem. B **107**, 8654 (2003).

[58] M. T. Zanni, S. Gnanakaran, J. Stenger, and R. M. Hochstrasser, J. Phys. Chem. B **105**, 6520 (2001).

[59] I. V. Rubtsov and R. M. Hochstrasser, J. Phys. Chem. B **106**, 9165 (2002).

[60] K. A. Merchant, W. G. Noid, R. Akiyama, I. J. Finkelstein, A. Goun, B. L. McClain, R. F. Loring, and M. D. Fayer, J. Am. Chem. Soc. **125**, 13804 (2003).

[61] H. S. Chung, M. Khalil, and A. Tokmakoff, J. Phys. Chem. B **108**, 15332 (2004).

[62] N. Demirdöven, C. M. Cheatum, H. S. Chung, M. Khalil, J. Knoester, and A. Tokmakoff, J. Am. Chem. Soc. **126**, 7981 (2004).

[63] A. M. Massari, I. J. Finkelstein, B. L. McClain, A. Goj, X. Wen, K. L. Bren, R. F. Loring, and M. D. Fayer, J. Am. Chem. Soc. **127**, 14279 (2005).

[64] S. Woutersen, G. S. Y. Mu, and P. Hamm, Chem. Phys. **266**, 137 (2001).

[65] J. B. Asbury, T. Steinel, and M. Fayer, J. Lumin. **107**, 271 (2004).

[66] J. B. Asbury, T. Steinel, and M. Fayer, J. Phys. Chem. B **108**, 6544 (2004).

[67] I. V. Rubtsov, K. Kumar, and R. M. Hochstrasser, Chem. Phys. Lett. **402**, 439 (2005).

[68] J. B. Asbury, T. Steinel, C. Stromberg, S. A. Corcelli, C. P. Lawrence, J. L. Skinner, and M. D. Fayer, J. Phys. Chem. A **108**, 1107 (2004).

[69] E. C. Fulmer, F. Ding, and M. T. Zanni, J. Chem. Phys. **122**, 034302 (2005).

[70] F. Ding, E. C. Fulmer, and M. T. Zanni, J. Chem. Phys. **123**, 094502 (2005).

[71] E. C. Fulmer, F. Ding, P. Mukherjee, and M. T. Zanni, Phys. Rev. Lett. **94**, 067402 (2005).

[72] W. G. Rothschild, J. Chem. Phys. **65**, 455 (1976).

[73] A. O. Caldeira and A. J. Leggett, Ann. Phys. (N.Y.) **149**, 374 (1983).

[74] U. Weiss, *Quantum Dissipative Systems*, 2nd ed. (World Scientific, Singapore, 1999).

[75] Y. Tanimura and P. G. Wolynes, Phys. Rev. A **43**, 4131 (1991).

[76] A. Ishizaki and Y. Tanimura, J. Phys. Soc. Jpn. **74**, 3131 (2005).

[77] R. Zwanzig, *Nonequillibrium Statistical Mechanics* (Oxford University Press, New York, 2001).

[78] A. O. Caldeira and A. J. Leggett, Physica A **121**, 587 (1983).

[79] M. Tuckerman and B. J. Berne, J. Chem. Phys. **98**, 7301 (1993).

[80] R. B. Williams and R. F. Loring, J. Chem. Phys. **113**, 10651 (2000).

[81] K. Okumura and Y. Tanimura, Phys. Rev. E **56**, 2747 (1997).

[82] T. Kato and Y. Tanimura, J. Chem. Phys. **117**, 6221 (2002).

[83] Y. Tanimura and R. Kubo, J. Phys. Soc. Jpn. **58**, 101 (1989).

[84] R. P. Feynman and F. L. Vernon, Ann. Phys. (N.Y.) **24**, 118 (1963).

[85] R. P. Feynman and A. R. Hibbs, *Quantum Mechanics and Path Integrals* (McGraw-Hill, New York, 1965).

[86] E. B. Davies, *Quantum Theory of Open Systems* (Academic, London, 1976).

[87] M. Khalil, N. Demirdöven, and A. Tokmakoff, Phys. Rev. Lett. **90**, 047401 (2003).